



## **Main Manuscript for**

### **COVID-19 lockdowns cause global air pollution declines**

Zander S. VENTER<sup>1\*</sup>; Kristin AUNAN<sup>2</sup>; Sourangsu CHOWDHURY<sup>3</sup>; Jos LELIEVELD<sup>3,4</sup>

<sup>1</sup> Terrestrial Ecology Section, Norwegian Institute for Nature Research - NINA, 0349 Oslo, Norway

<sup>2</sup> CICERO Center for International Climate Research, PO Box 1129 Blindern, 0318 Oslo, Norway

<sup>3</sup> Department of Atmospheric Chemistry, Max Planck Institute for Chemistry, 55128 Mainz, Germany

<sup>4</sup> Climate and Atmosphere Research Center, The Cyprus Institute, 1645 Nicosia

\* Zander Venter

**Email:** [zander.venter@nina.no](mailto:zander.venter@nina.no)

<https://orcid.org/0000-0003-2638-7162> (ZSV)

<https://orcid.org/0000-0002-7865-9134> (KA)

<https://orcid.org/0000-0002-4600-2226> (SC)

<https://orcid.org/0000-0001-6307-3846> (JL)

#### **Classification**

Physical science / Earth, Atmospheric and Planetary Sciences

Social Sciences / Environmental Sciences

#### **Keywords**

*Air quality, COVID-19 confinement, Emissions, Nitrogen dioxide, Particulate matter, Public health*

## Author Contributions

ZSV: concept, data analysis and writing. KA, SC, JL: concept, manuscript review.

## This PDF file includes:

Main Text  
Figures 1 to 5

## Abstract

The lockdown response to COVID-19 has caused an unprecedented reduction in global economic and transport activity. We test the hypothesis that this has reduced tropospheric and ground-level air pollution concentrations using satellite data and a network of >10000 air quality stations. After accounting for the effects of meteorological variability, we find declines in the population-weighted concentration of ground-level nitrogen dioxide (NO<sub>2</sub>: 60% with 95% confidence interval 48% to 72%), and fine particulate matter (PM<sub>2.5</sub>: 31%; 17% to 45%), with marginal increases in ozone (O<sub>3</sub>: 4%; -2% to 10%) in 34 countries during lockdown dates up until 15 May. Except for ozone, satellite measurements of the troposphere indicate much smaller reductions, highlighting the spatial variability of pollutant anomalies attributable to complex NO<sub>x</sub> chemistry and long-distance transport of PM<sub>2.5</sub>. By leveraging Google and Apple mobility data, we find some of the first empirical evidence for a link between global vehicle transportation declines and the reduction of ambient NO<sub>2</sub> exposure. While the state of global lockdown is not sustainable, these findings allude to the potential for mitigating public health risk by reducing “business as usual” air pollutant emissions from economic activities. Explore trends here:

<https://nina.earthengine.app/view/lockdown-pollution>

## Significance Statement

The global response to the COVID-19 pandemic has resulted in unprecedented reductions in economic activity. We find that, after accounting for meteorological variations, lockdown events have reduced the population-weighted concentration of nitrogen dioxide and particulate matter levels by about 60% and 31% in 34 countries with mixed effects on ozone. Reductions in transportation sector emissions are largely responsible for the NO<sub>2</sub> anomalies.

## Main Text

### Introduction

In many developing nations economic growth has exacerbated air pollutant emissions with severe consequences for the environment and human health. Long-term exposure to air pollution including fine particulate matter with a diameter less than 2.5 μm (PM<sub>2.5</sub>) and ozone (O<sub>3</sub>) are estimated to cause ~8.8 million excess deaths annually (1, 2), while nitrogen dioxide (NO<sub>2</sub>) results in 4 million new pediatric asthma cases annually (3). Despite the apparent global air pollution “pandemic”, anthropogenic emissions continue to increase in most developing and some developed nations (4–6).

The major ambient (outdoor) air pollution sources include power generation, industry, traffic, and residential energy use (4, 7). With the rapid emergence of the novel coronavirus (COVID-19), and in particular the government enforced lockdown measures aimed at containment, economic activity associated with transport and mobility has come to a near-complete standstill in many countries (8). Lockdown measures have included partial or complete closure of international borders, schools, non-essential businesses and in some cases restricted citizen mobility (SI

Appendix, Fig. S1) (9). The associated reduction in traffic and industry has both socio-economic and environmental impacts which are yet to be quantified. In parallel to the societal consequences of the global response to COVID-19, there is an unprecedented opportunity to estimate the short-term effects of economic activity counterfactual to “business as usual” on global air pollution and its relation to human health.

Here we test the hypothesis that COVID-19 lockdown events between January and the middle of May 2020 were associated with declines in ambient NO<sub>2</sub>, O<sub>3</sub>, and PM<sub>2.5</sub> air pollutant concentrations. Country-specific lockdowns are defined by the average date of policy restrictions on mobility, workplace closure and stay-at-home advisories (10). We use satellite data to provide a global perspective of atmospheric pollutant dynamics, but to quantify air pollution anomalies relevant to public health, we utilize ground-level measurements from >10000 air quality stations in 34 countries after accounting for meteorological variations.

## **Results and Discussion**

### ***General air pollution changes***

Before accounting for meteorological variability, we observed declines in ground-level NO<sub>2</sub> (36% population-weighted mean with interquartile range; IQR: 26%) and PM<sub>2.5</sub> (31%; IQR: 50%) concentrations recorded by air quality stations across 34 countries during 2020 (01-Jan to 15-May) relative to a 3-yr average for the same dates (Fig. 1). In contrast, O<sub>3</sub> increased by 105% (77% IQR). Satellite measurements of tropospheric pollutant concentrations over the inhabited areas also reveal declines in NO<sub>2</sub> (15%; IQR: 27%) and increases in O<sub>3</sub> (4%; IQR: 6%; SI Appendix, Fig. S3 & S4) relative to 2019 averages. Measures of aerosol optical depth (AOD, a proxy for PM<sub>2.5</sub>) declined by 4.7% (35% IQR). Therefore ground-level and total column tropospheric trends in pollutants show a correspondence in the direction of change but not necessarily the magnitude of change. This is likely because tropospheric pollutant concentrations may be significantly diluted relative to ground-level concentrations due to mixing and transport in meso-scale weather systems. This is particularly likely because the satellite data have not been adjusted for confounding meteorological effects. For instance, elevated AOD may be a product of long-distance aerosol transport and not ground-level sources of PM<sub>2.5</sub> (11). The same is true for satellite-measured O<sub>3</sub>, which is strongly influenced by its generally increasing abundance above the boundary layer, especially during winter.

The simple comparison of 2020 January-May averages to 3- or 1-yr baseline values (Fig. 1, SI Appendix, Fig. S3 & S4) does not isolate the COVID-19 lockdown effect for two reasons. Firstly, lockdowns were implemented over different dates across the globe and therefore averaging over January-May smooths over the country-specific lockdown effects. Secondly, local up to synoptic scale weather patterns (temperature, humidity, precipitation, vertical mixing and advection) can significantly affect ground-level pollutant concentrations (12, 13). Although measuring 2020 changes relative to previous years partially controls for this, it does not fully account for anomalous weather during 2020 that may have confounded any observable effect of COVID-19 lockdowns. Therefore, we used historical relationships between weather and daily pollutant time series in a regression model to estimate what the pollutant levels would have been during lockdown dates. The COVID-19 lockdown effect was then defined as the difference between observed and weather benchmark pollutant levels (SI Appendix, Fig. S2). We used ground-level measurements because

they are more sensitive to emission source changes and are more relevant to human exposure and health risk.

### ***Weather-corrected air pollution changes during lockdown***

As of 15 May 2020, the 34 countries considered had been in lockdown for an average of 62 days, with China (113 days) and Italy (84 days) undergoing the longest lockdowns and Mexico undergoing the shortest (50 days; SI Appendix, Fig. S1). During lockdown dates, ground-level NO<sub>2</sub> concentrations were on average 60% (population-weighted mean with 95% confidence intervals: 48% to 72%) lower than those we would have expected given the prevailing weather and time of year (weather-corrected benchmark; Fig. 2A & 3A). Similarly, PM<sub>2.5</sub> declined by 31% (17% to 45%), whereas O<sub>3</sub> increased by 4% (-2% to 10%; Fig 2 & 3). In absolute terms (Fig. 3A), this equates to a 11 µg m<sup>-3</sup> (9 to 14 µg m<sup>-3</sup>) decline in NO<sub>2</sub> and a 12 µg m<sup>-3</sup> (7 to 18 µg m<sup>-3</sup>) decline in PM<sub>2.5</sub>. The 4 µg m<sup>-3</sup> increase in O<sub>3</sub> (1 to 8 µg m<sup>-3</sup>) was lower in magnitude and less significant. These results mirror the direction of change found in the general trends for uncorrected ground-level (Fig. 1) and satellite-derived pollutant dynamics (SI Appendix, Fig. S3 & S4). They also corroborate preliminary (not peer-reviewed) findings from studies in China (14), Spain (15), and the USA (16) which have documented local declines in pollutant concentrations during lockdown.

Globally, the timing of the deviation from benchmark levels for NO<sub>2</sub> was remarkably coincident with the start of lockdown (Fig. 2; SI Appendix, Fig. S5). This timing was strongly evident for PM<sub>2.5</sub> in China (decline of 16 µg m<sup>-3</sup>) and India (decline of 15 µg m<sup>-3</sup>), but less so for PM<sub>2.5</sub> over European countries. This may be because PM<sub>2.5</sub> is significantly influenced by long-distance atmospheric transport and therefore the local effects of economic activity over Europe may have been diluted or even counteracted (17). As an example, in March easterly winds carried desert dust across Europe from West Asia, which resulted in a temporal increase of AOD (18). Moreover, some PM<sub>2.5</sub> sources including agriculture and energy production were not disrupted by lockdown policy restrictions. This is also evidenced in the two notable outlier countries exhibiting increases in PM<sub>2.5</sub>, namely Thailand and Australia (Fig. 3). There the increases are largely attributable to the recent wildfires and associated smoke aerosol levels that have overwhelmed the effect of reduced economic and transport activity (19, 20).

We find that the global NO<sub>2</sub> and PM<sub>2.5</sub> anomalies associated with lockdowns normalized after about two months (Fig. 2). This normalization occurred in early April over China (SI Appendix, Fig. S5) which is consistent with the release of lockdown on 8 April over Wuhan province, the epicenter of the COVID-19 pandemic. NO<sub>2</sub> concentrations normalized during late April and early May over European countries including Italy, Spain and the United Kingdom (SI Appendix, Fig. S5). This is likely a signal of increasing economic activity coincident with the gradual easing of lockdown restrictions around the world after countries have successfully “flattened the curve” of COVID-19 infections (21).

### ***Explaining the spatial variation in change***

Despite the overall average decline in air pollution during lockdown, there was substantial variation between countries both in terms of the direction and magnitude of change (Fig. 3). The declines in NO<sub>2</sub> were relatively ubiquitous over space (28 out of 34 countries; Fig. 3), however O<sub>3</sub> and PM<sub>2.5</sub> anomalies were more variable. We posit that this spatial variation is likely due to a combination of (1) unaccounted for meteorological and environmental factors that affect ambient air pollution chemistry, or (2) country-specific differences the way lockdown regulations influenced pollution emission sources across economic sectors.

Our weather benchmark models were not able to explain all of the temporal variance in NO<sub>2</sub> (R<sup>2</sup> = 0.52), O<sub>3</sub> (R<sup>2</sup> = 0.59), and PM<sub>2.5</sub> (R<sup>2</sup> = 0.34; SI Appendix, Table S1). This is not surprising given that pollutants like O<sub>3</sub> are affected by non-linear chemical interactions with volatile organic

compounds (VOCs) and  $\text{NO}_x$ , mediated by mesoscale and urban canopy circulation patterns (22). For instance, the emission decline of  $\text{NO}_x$  ( $=\text{NO}+\text{NO}_2$ ), mostly as NO, could lead to reduced local titration of  $\text{O}_3$  (reaction of NO with  $\text{O}_3$ ). The  $\text{O}_3$  titration effect is relevant locally and within the planetary boundary layer, whereas further downwind photochemical  $\text{O}_3$  formation, with a catalytic role of  $\text{NO}_x$ , is a more important factor. For example, in China, the population-weighted  $\text{O}_3$  is found to increase with decreasing  $\text{NO}_2$  across the lockdown, this indicates predominance of VOC-limited regime in China. Whereas, reduction in population-weighted  $\text{O}_3$  with decrease in  $\text{NO}_2$  in India suggests a  $\text{NO}_x$ -limited regime prevailing there (Fig. S5). Note that lockdown impacts on  $\text{NO}_2$ , which has an atmospheric lifetime of about a day, are clearly discernible locally, whereas those on  $\text{O}_3$  with a lifetime of several weeks are affected by long-distance transport associated with specific weather patterns. Further,  $\text{O}_3$  photochemistry in temperate latitudes during the Feb/Mar period is still slow due to low solar irradiation, whereas at lower latitudes pollutant  $\text{O}_3$  buildup can be significant.

The alternative explanation for the spatial variability in pollutant changes during lockdown is that confinement regulations had varying effects on emission sources between countries. Recent analysis of the 17% decline in  $\text{CO}_2$  emissions during lockdowns have indicated substantial variability between economic sectors (23), with the largest declines taking place in the surface transport sector. Sector allocations of  $\text{CO}_2$  emissions vary between countries. For example, the transport sector contributes 8% toward  $\text{CO}_2$  emissions in China, whereas in the United Kingdom allocation is four times higher (23). Therefore, one might expect large variations in emission declines (particularly for  $\text{NO}_2$ ) between countries given that the lockdowns brought about the greatest change in the transportation sector.

We explored nationally aggregated citizen mobility datasets published by Google (<https://www.google.com/covid19/mobility/>) and Apple (<https://www.apple.com/covid19/mobility/>) and found a significant association between country-specific  $\text{NO}_2$  declines and reductions in work commutes ( $p < 0.05$ ; Fig. 4A) and vehicle driving activity ( $p < 0.05$ ; Fig. 4B). There were no significant relationships for  $\text{O}_3$  and  $\text{PM}_{2.5}$  anomalies. This suggests  $\text{NO}_2$  has a stronger coupling to land-transportation and small business activity declines during lockdown compared to  $\text{O}_3$  and  $\text{PM}_{2.5}$ . In many countries  $\text{PM}_{2.5}$  is more strongly linked to residential energy use, power generation and agriculture (7). Given that walking and cycling are attributes of social distancing measures (24) that are expected to continue for some time (25), reduced  $\text{NO}_2$  emissions and therefore exposure levels may be sustained over the near future.

## Implications

Reducing economic activity to levels equivalent to a lockdown state may be impractical, yet maintaining “business as usual” clearly exacerbates global pollutant emissions and ambient exposure levels. Our study documents the dramatic short-term effect of global reductions in transport and economic activity on reducing ground-level  $\text{NO}_2$  and  $\text{PM}_{2.5}$ , with mixed effects on  $\text{O}_3$  concentrations. Short-term epidemiological analyses suggest that pollutant reductions may have offset COVID-19 deaths (14, 26, 27), however the full extent to which this is true remains to be seen. In some settings where household (indoor) air pollution from solid fuel use is widespread, overall exposure may have increased as a result of lockdown policies (28). As the pandemic plays out, empirical data will emerge to fill in the knowledge gaps and uncertainties associated with the air pollution health burden attribution. Nevertheless, finding means to curb air pollutant emissions remains important and here we provide some of the first empirical evidence at a global scale for a coupling between vehicle transport reduction and declining ambient  $\text{NO}_2$  concentrations. This provides justification for city-level initiatives to promote public transport systems as well as pedestrian and cycling activity. Finding economically and socially sustainable alternatives to fossil fuel use in industries, transportation and power plants, and cleaner fuels for

use in households are additional means of reaching the pollutant declines we have observed during the global response to COVID-19 (29, 30).

## **Materials and Methods**

In brief, the methodological workflow (SI Appendix, Fig. S2) described below involves collecting satellite and ground station air pollution time series data to estimate anomalies during the 2020 COVID-19 period relative to different baseline levels. We collect satellite data to provide a global perspective of pollutant trends over regions where there is a scarcity of ground air quality stations. However, we focus on weather-corrected ground station data because ambient pollutant concentrations are more relevant to public health than satellite-derived tropospheric column concentrations. Regression models are used to correct for the potential effects of weather-related variations on ground-level pollutant levels during lockdown. The sample of countries used in each step varies dependent on the data availability. Results for ground-station data cover 34 countries while satellite data cover 48 countries.

### ***Satellite data***

All remote sensing data analyses were conducted in the Google Earth Engine platform for geospatial analysis and cloud computing (31). All data was extracted at a global scale and aggregated to the population-weighted mean for each country. Population data were obtained for 2020 from the Gridded Population of the World v4 dataset (32). Data outside of inhabited areas (ocean, freshwater, desert etc.) were excluded from the analysis using the Global Human Settlement Layer produced by the European Joint Research Centre which defines inhabited rural and urban terrestrial areas (33). We did this because our main hypothesis was linked to human exposure and therefore we aimed at pollution measures that were relevant to inhabited land surfaces.

We collected nitrogen dioxide (NO<sub>2</sub>) and ozone (O<sub>3</sub>) data from the TROPOspheric Monitoring Instrument (TROPOMI), on-board the Sentinel-5 Precursor satellite (34). TROPOMI has delivered calibrated data since July 2018 from its nadir-viewing spectrometer measuring reflected sunlight in the visible, near-infrared, ultraviolet, and shortwave infrared. Recent work has shown that TROPOMI measurements are well correlated to ground measures of NO<sub>2</sub> (35, 36). We filtered out pixels that are fully or partially covered by clouds using 0.3 as a cutoff for the radiative cloud fraction. As a proxy for atmospheric fine particulate matter (PM<sub>2.5</sub>), we collected aerosol optical depth (AOD) data from the cloud-masked MCD19A2.006 Terra and Aqua MAIAC collection (37). This dataset has been successfully used to map ground-level PM<sub>2.5</sub> concentrations (38, 39). Global median composite images for NO<sub>2</sub>, O<sub>3</sub> and AOD were then calculated for the months of January to May in 2019 and 2020.

### ***Ground station data***

Although satellite data have the advantage of wall-to-wall global coverage, there are some drawbacks: (1) TROPOMI does not extend back far enough to obtain an adequate baseline measure with which to compare 2020 concentrations; (2) MODIS and TROPOMI collect information within either the total (O<sub>3</sub> and AOD) or tropospheric (NO<sub>2</sub>) column which do not necessarily reflect pollutant levels experienced on the ground. Therefore, we also collected NO<sub>2</sub>, O<sub>3</sub> and PM<sub>2.5</sub> data from >10000 in-situ air quality monitoring stations to supplement the satellite data. These data were accessed from the OpenAQ Platform and originate from government- and research-grade sources. See [www.openaq.org](http://www.openaq.org) for a list of sources. Despite the reliability of the sources, we inspected pollutant time series for each country and removed spurious outliers in the data with z-scores (40) exceeding an absolute value of 3 (within three standard deviations from

the mean). Following quality control, we were left with data representing 34 countries. When aggregating data to country level, we used population-weighted means based on the population density within 10 km of each ground station.

### ***Quantifying air pollution anomalies***

We used two approaches to quantify air pollution anomalies coincident with COVID-19 during January to May 15, 2020. We refer to these as (1) the Jan-May differential, and (2) the lockdown differential (SI Appendix, Fig. S2). For the Jan-May differential we calculated average pollutant levels for Jan-May each year between 2017 and 2020. The differential was defined as the difference between 2020 values and the average of those for a 3-year baseline (2017-2019). For satellite data the baseline was the 2019 Jan-May average due to limited temporal extent of TROPOMI data, however for ground-stations we considered a 3-year (2017-2019) average for the Jan-May period.

Air pollution anomalies measured with the Jan-May differential approach may smooth over the effect of COVID-19 given that country-specific lockdowns or mitigation actions occurred at different times. For instance, China went into lockdown in January whereas the majority of lockdowns in other countries occurred in March (SI Appendix, Fig. S1). Therefore, we attempted to isolate the effect of COVID-19 mitigation measures by calculating lockdown pollutant levels for each country separately. We utilized a dataset that consolidates national policy regulations relating to COVID-19 confinement measures (10). The start of lockdown was calculated separately for each country as the average date on which policies for stay-at-home restrictions, mobility restrictions, and workplace closures were announced (SI Appendix, Fig. S1).

Air pollution anomalies measured during lockdowns are not necessarily attributable to reduced economic activity, but may be an artifact of meteorological variability coincident with the onset of COVID-19. Therefore, we adopted a weather benchmark modelling approach to predict what the expected air pollution levels for 2020 lockdown dates should have been given the prevailing weather conditions and time of year. We used multiple linear regression as a modelling framework after testing both Random Forest and generalized linear models which had lower predictive accuracy based on assessing model performance by predicting against a withheld validation dataset. We built separate linear regression models for each country and pollutant type, where daily pollutant concentrations were regressed on a number of explanatory variables including: temperature, humidity, precipitation, wind speed, day of year, day of week, week of year and month of year. Weather data were downloaded from the Global Forecast System (GFS) of the National Centers for Environmental Prediction (NCEP) between Jan 2017 and May 15, 2020. We calculated the *sin* and *cos* component of the day, week and month variables to account for their cyclical nature. Using models trained on historical data (before 1 January 2020), we predicted the expected pollutant levels for lockdown dates. The modelled differential is then the difference between this predicted benchmark value and the observed pollutant concentrations during lockdown (SI Appendix, Fig. S2). This differential can be attributed to COVID-19 mitigation measures with greater confidence than simple comparisons with 3-yr baseline values.

### ***Data availability***

Data and scripts used to produce this analysis are available at this GitHub repository: <https://github.com/NINAnor/covid19-air-pollution>

### **Acknowledgments**

Thanks to Samantha Scott Venter for assistance with collection of country-specific lockdown data. Thanks to the OpenAQ community for making air quality data open-access. KA was supported by funding from the European Union's Horizon 2020 research and innovation programme under grant agreement No 820655 (EXHAUSTION). We are grateful for the effort contributed by the reviewers towards improving the manuscript.

## References

1. R. Burnett, *et al.*, Global estimates of mortality associated with long-term exposure to outdoor fine particulate matter. *Proc. Natl. Acad. Sci.* **115**, 9592–9597 (2018).
2. J. Lelieveld, *et al.*, Loss of life expectancy from air pollution compared to other risk factors: a worldwide perspective. *Cardiovasc. Res.* (2020) <https://doi.org/10.1093/cvr/cvaa025> (March 30, 2020).
3. P. Achakulwisut, M. Brauer, P. Hystad, S. C. Anenberg, Global, national, and urban burdens of paediatric asthma incidence attributable to ambient NO<sub>2</sub> pollution: estimates from global datasets. *Lancet Planet. Health* **3**, e166–e178 (2019).
4. M. Crippa, *et al.*, Gridded emissions of air pollutants for the period 1970–2012 within EDGAR v4.3.2. *Earth Syst. Sci. Data* **10**, 1987–2013 (2018).
5. R. M. Hoesly, *et al.*, Historical (1750–2014) anthropogenic emissions of reactive gases and aerosols from the Community Emissions Data System (CEDS). *Geosci. Model Dev.* **11**, 369–408 (2018).
6. C. Li, *et al.*, India Is Overtaking China as the World's Largest Emitter of Anthropogenic Sulfur Dioxide. *Sci. Rep.* **7**, 1–7 (2017).
7. J. Lelieveld, J. S. Evans, M. Fnais, D. Giannadaki, A. Pozzer, The contribution of outdoor air pollution sources to premature mortality on a global scale. *Nature* **525**, 367–371 (2015).
8. J. Cohen, K. Kupferschmidt, Strategies shift as coronavirus pandemic looms. *Science* **367**, 962–963 (2020).
9. E. Pepe, *et al.*, COVID-19 outbreak response: a first assessment of mobility changes in Italy following national lockdown. *medRxiv*, 2020.03.22.20039933 (2020).
10. T. Hale, S. Webster, A. Petherick, T. Phillips, B. Kira, Oxford COVID-19 Government Response Tracker (2020).
11. Convention on Long-range Transboundary Air Pollution, United Nations, F. Dentener, T. Keating, H. Akimoto, *Hemispheric transport of air pollution 2010: Part A-ozone and particulate matter* (UN, 2010).
12. J. Dawson, Quiet weather, polluted air. *Nat. Clim. Change* **4**, 664–665 (2014).
13. D. J. Jacob, D. A. Winner, Effect of climate change on air quality. *Atmos. Environ.* **43**, 51–63 (2009).
14. K. Chen, M. Wang, C. Huang, P. L. Kinney, P. T. Anastas, Air pollution reduction and mortality benefit during the COVID-19 outbreak in China. *Lancet Planet. Health* **0** (2020).



15. A. Tobías, *et al.*, Changes in air quality during the lockdown in Barcelona (Spain) one month into the SARS-CoV-2 epidemic. *Sci. Total Environ.*, 138540 (2020).
16. B. Bekbulat, *et al.*, PM2.5 and Ozone Air Pollution Levels Have Not Dropped Consistently Across the US Following Societal Covid Response (2020) <https://doi.org/10.26434/chemrxiv.12275603.v2> (May 26, 2020).
17. R. B. Khuzestani, *et al.*, Quantification of the sources of long-range transport of PM2.5 pollution in the Ordos region, Inner Mongolia, China. *Environ. Pollut.* **229**, 1019–1031 (2017).
18. X. Querol, *et al.*, Monitoring the impact of desert dust outbreaks for air quality for health studies. *Environ. Int.* **130**, 104867 (2019).
19. C. E. Reid, *et al.*, Associations between respiratory health and ozone and fine particulate matter during a wildfire event. *Environ. Int.* **129**, 291–298 (2019).
20. S. Sambhi, Forest fires rage in northern Thailand. *Eco-Bus.* (2020) (May 24, 2020).
21. A. P. Balasa, COVID – 19 on Lockdown, Social Distancing and Flattening the Curve – A Review. *Eur. J. Bus. Manag. Res.* **5** (2020).
22. M. E. Marlier, A. S. Jina, P. L. Kinney, R. S. DeFries, Extreme Air Pollution in Global Megacities. *Curr. Clim. Change Rep.* **2**, 15–27 (2016).
23. C. Le Quéré, *et al.*, Temporary reduction in daily global CO<sub>2</sub> emissions during the COVID-19 forced confinement. *Nat. Clim. Change*, 1–7 (2020).
24. Z. Venter, D. Barton, V. Gundersen, H. Figari, M. Nowell, Urban nature in a time of crisis: recreational use of green space increases during the COVID-19 outbreak in Oslo, Norway. *SocArXiv* (2020) <https://doi.org/doi:10.31235/osf.io/kbdum>.
25. S. M. Kissler, C. Tedijanto, E. Goldstein, Y. H. Grad, M. Lipsitch, Projecting the transmission dynamics of SARS-CoV-2 through the postpandemic period. *Science* **368**, 860–868 (2020).
26. E. Conticini, B. Frediani, D. Caro, Can atmospheric pollution be considered a co-factor in extremely high level of SARS-CoV-2 lethality in Northern Italy? *Environ. Pollut.*, 114465 (2020).
27. X. Wu, R. C. Nethery, B. M. Sabath, D. Braun, F. Dominici, Exposure to air pollution and COVID-19 mortality in the United States. *medRxiv*, 2020.04.05.20054502 (2020).
28. H. Shen, *et al.*, Increased air pollution exposure among the Chinese population during the national quarantine in 2020 (2020).
29. J. Lelieveld, *et al.*, Effects of fossil fuel and total anthropogenic emission removal on public health and climate. *Proc. Natl. Acad. Sci.* **116**, 7192–7197 (2019).
30. S. Chowdhury, *et al.*, Indian annual ambient air quality standard is achievable by completely mitigating emissions from household sources. *Proc. Natl. Acad. Sci.* **116**, 10711 (2019).
31. N. Gorelick, *et al.*, Google Earth Engine: Planetary-scale geospatial analysis for everyone. *Remote Sens. Environ.* **202**, 18–27 (2017).

32. Center for International Earth Science Information Network - CIESIN - Columbia University, Gridded Population of the World, Version 4 (GPWv4): Population Density, Revision 11 (2018).
33. M. Pesaresi, S. Freire, GHS Settlement grid following the REGIO model 2014 in application to GHSL Landsat and CIESIN GPW v4-multitemporal (1975-1990-2000-2015). *JRC Data Cat.* (2016).
34. J. P. Veefkind, *et al.*, TROPOMI on the ESA Sentinel-5 Precursor: A GMES mission for global observations of the atmospheric composition for climate, air quality and ozone layer applications. *Remote Sens. Environ.* **120**, 70–83 (2012).
35. D. Griffin, *et al.*, High-Resolution Mapping of Nitrogen Dioxide With TROPOMI: First Results and Validation Over the Canadian Oil Sands. *Geophys. Res. Lett.* **46**, 1049–1060 (2019).
36. A. Lorente, *et al.*, Quantification of nitrogen oxides emissions from build-up of pollution over Paris with TROPOMI. *Sci. Rep.* **9**, 1–10 (2019).
37. A. Lyapustin, Y. Wang, S. Korkin, D. Huang, MODIS Collection 6 MAIAC algorithm. *Atmospheric Meas. Tech.* **11**, 5741–5765 (2018).
38. Y. Zheng, Q. Zhang, Y. Liu, G. Geng, K. He, Estimating ground-level PM<sub>2.5</sub> concentrations over three megalopolises in China using satellite-derived aerosol optical depth measurements. *Atmos. Environ.* **124**, 232–242 (2016).
39. S. Chowdhury, *et al.*, Tracking ambient PM<sub>2.5</sub> build-up in Delhi national capital region during the dry season over 15 years using a high-resolution (1 km) satellite aerosol dataset. *Atmos. Environ.* **204**, 142–150 (2019).
40. D. Cousineau, S. Chartier, Outliers detection and treatment: a review. *Int. J. Psychol. Res.* **3**, 58–67 (2010).

## Figures and Tables

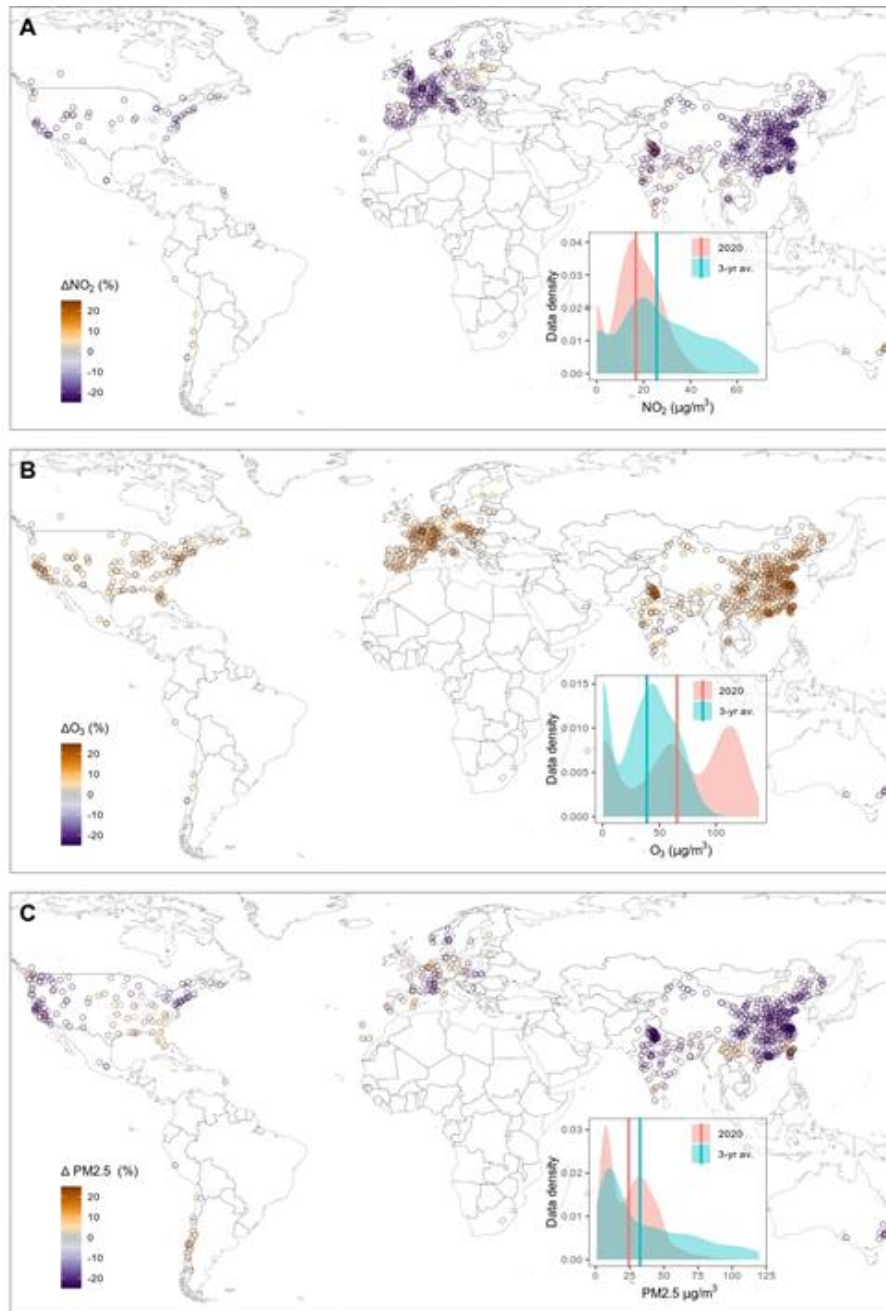


**Figure 1. Global distribution of 2020 ground-level air pollution anomalies.** Ground station measures of  $\text{NO}_2$  (A),  $\text{O}_3$  (B), and  $\text{PM}_{2.5}$  (C) anomalies are mapped. Anomalies are defined as deviations in 2020 Jan-May averages from 3-yr baseline levels for the same dates and are not corrected for weather variability. Inset plots show data density distributions for baseline and 2020 periods with median values as vertical lines.

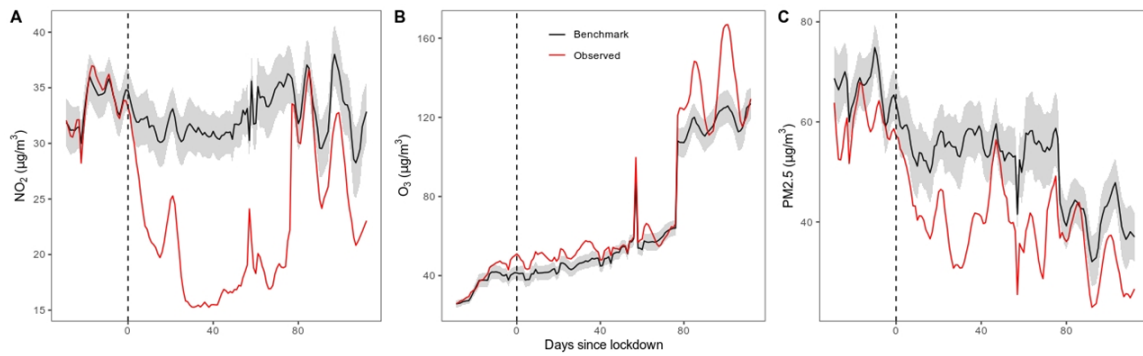


**Figure 2. Lockdown ground-level air pollution anomalies relative to weather benchmarks.** The daily population-weighted average ( $n = 34$  countries) ambient pollutant concentrations observed one month before and up to 15 May after lockdowns are plotted in red. Benchmark levels which represent expected concentrations considering time of year and prevailing weather are plotted in black with 95% confidence intervals.

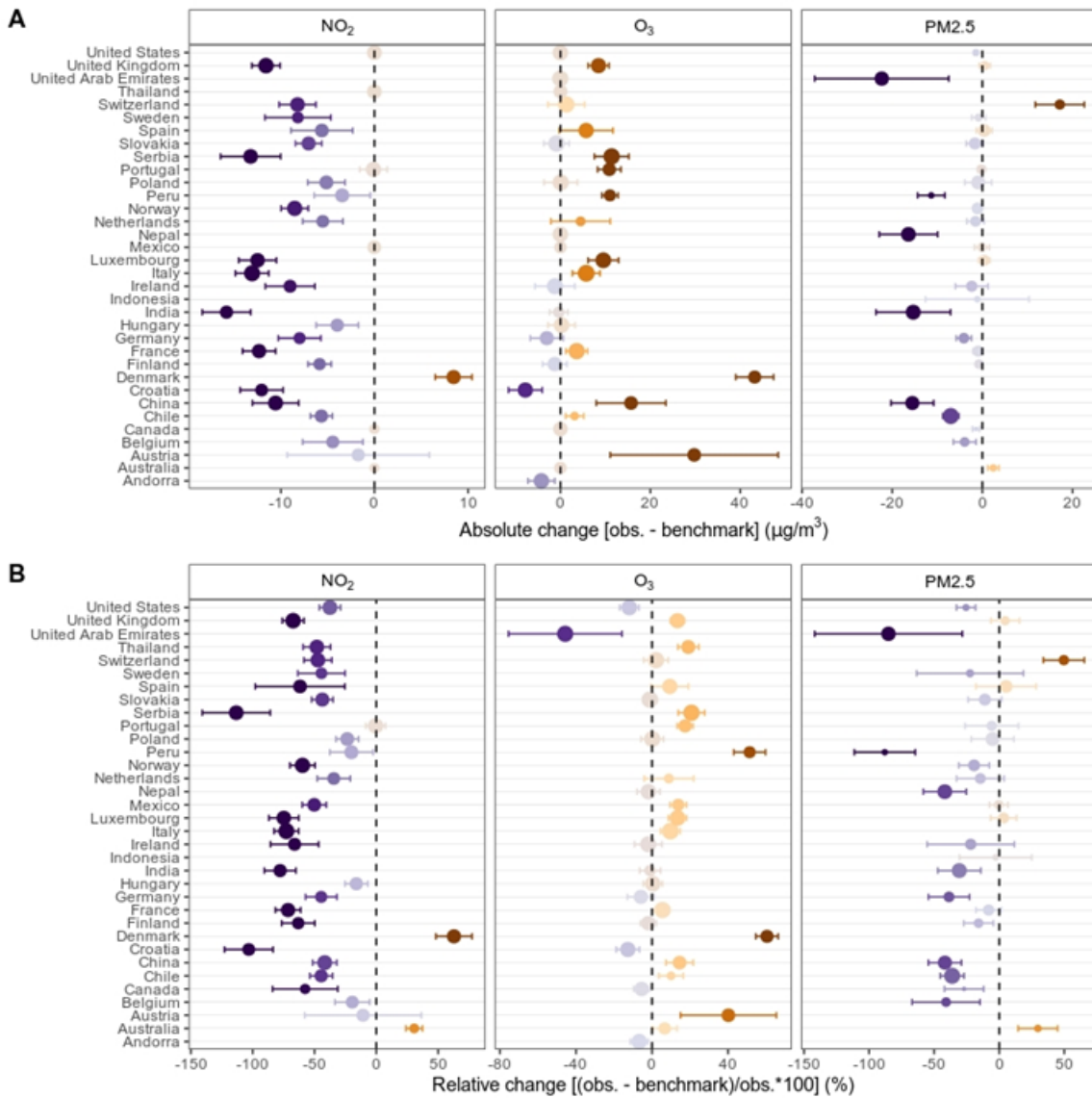


**Figure 3. Country-specific ground-level lockdown air pollution anomalies.** The difference between observed (obs.) lockdown ambient pollutant concentrations and those predicted by the weather benchmark model (trained on 2017-2019 data) are plotted for 34 countries (points) with 95% confidence intervals (error bars). Larger points represent regression models with greater  $R^2$  values. Both absolute (A) and relative (B) changes are presented.

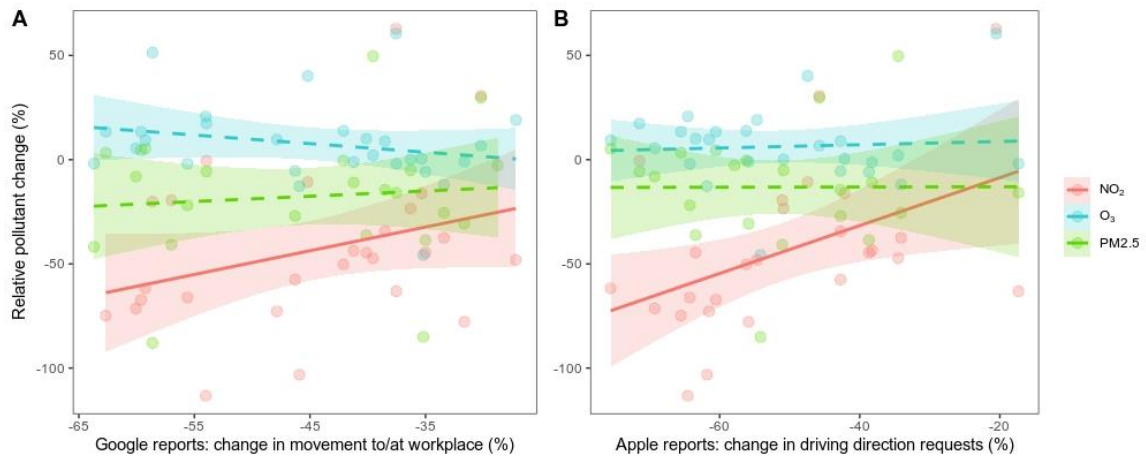


**Figure 4. Lockdown mobility changes relative to ground-level air pollution anomalies.** Country-specific ambient air pollution anomalies (observed relative to weather benchmark levels) are regressed on two measures of lockdown-induced citizen mobility declines. Significant (solid) and non-significant (dashed) linear regression lines are plotted for each pollutant. Each point represents a country's aggregated value (n = 34).